

# Pressure Drop of Fully Developed, Laminar Flow in Rough Microtubes

**M. Bahrami**

Post Doctoral Fellow

Mem. ASME

e-mail: majid@mhtlab.uwaterloo.ca

**M. M. Yovanovich**

Distinguished Professor Emeritus

Fellow ASME

**J. R. Culham<sup>1</sup>**

Associate Professor

Mem. ASME

Microelectronics Heat Transfer Laboratory,

Department of Mechanical Engineering,

University of Waterloo,

Waterloo, Ontario, Canada N2L 3G1

## 1 Introduction

Advances in fabrication methods in microelectromechanical systems (MEMS) have generated significant interest in the area of microscale heat transfer and fluid flow. Microchannel heat exchangers can dissipate high heat fluxes which make them well suited for a wide variety of unique cooling applications. Microchannels can also be integrated directly within the heat generating component; thus, the thermal contact resistance at the interface of a heat-generating component and heat sink is eliminated. This feature leads to lower substrate temperatures and smaller temperature gradients that make microchannels attractive for microelectronics cooling applications [1]. In addition, microchannels are being used in other applications, such as reactant delivery, physical particle separation, and inkjet print heads.

Microchannels can be defined as tubes/channels whose diameters are less than 1 mm. There are many techniques used to manufacture microchannels, but the following four processes are more common [2]: (i) Micromechanical machining, e.g., diamond machining, laser processes, microdrilling; (ii) x-ray machining (such as LIGA Lithographie-Galvanoforming-Abformung). (iii) photolithographic-based techniques such as Si chemical etching; and (iv) surface and surface-proximity micromachining.

Many researchers have conducted experiments and reported friction factors higher than the values predicted by conventional theory (smooth pipes) for liquids in microchannels during the last 15 years (see survey articles [1,2]). Tuckerman [3] was the first to experimentally investigate the liquid flow and heat transfer in microchannels. He reported that the flow approximately followed the Hagen-Poiseuille theory. Pfahler et al. [4,5] conducted experimental studies on the fluid flow in microchannels. They observed that in the relatively large channels, the experimental observations were in general agreement with the predictions from conventional equations. However, in the smallest of the channels, they observed a significant deviation from the classical predictions. Mala and Li [6] measured the friction factor of water in microtubes with diameters ranging from 50 to 254  $\mu\text{m}$ . They also reported good agreement with the classical theory in large diameters microtubes. They

proposed a roughness-viscosity model to explain the increase in the friction factor of the microchannels. The model of [6], however, did not encompass the physical mechanism and the effect of wall roughness. Li et al. [7] experimentally studied the frictional resistance for deionized water flow in microtubes. They reported a 15%–37% higher friction factor than the classical theory for rough microtubes. They concluded that the effect of wall roughness cannot be neglected for microtubes. However, they did not propose any models to explain the higher friction factors observed experimentally.

Kleinstreuer and Koo [8] proposed a computational model to consider the effect of wall roughness on liquid flow in microchannels. They modeled roughness by considering a *porous medium layer* (PML) near the wall. They showed good agreement with experimental data when the relative roughness was relatively large. The PML model of [8] requires parameters such as permeability and porosity for the “porous layer” which must be supplied to their numerical code. These parameters cannot be measured directly; no relationship was proposed for determining these parameters in [8].

As the diameter of (micro-) tubes decreases, the surface to volume ratio, which is equal to  $2/r$ , increases rapidly. As a result, the surface phenomena, including the effect of roughness, become more significant. There is a need for a better understanding of the effect of wall roughness on fluid characteristics in microtubes. This paper is the first attempt to develop an analytical model to predict the pressure drop of the fully developed, laminar, incompressible flows in rough microtubes.

## 2 Frictional Resistance

Consider *pressure-driven* flow in a long microtube. The Reynolds number associated with the flow is in general small, due to the small radii, therefore the flow is laminar. Applying a force balance and the no-slip boundary condition, one can find a relationship between the mass flow rate  $\dot{m}$ , and the pressure drop  $\Delta P$  for a smooth circular tube of radius  $a$ , as follows (Hagen-Poiseuille flow):

$$\dot{m} = \frac{\pi a^4 \rho \Delta P}{8 \mu L} \quad (1)$$

where the mean velocity of the fluid is,  $\bar{u} = \dot{m} / \pi \rho a^2$ . The relationship between the pressure gradient and the mean velocity is  $\Delta P / L = 8 \mu \bar{u} / a^2$ . It can easily be shown that  $f = 64 / \text{Re}_D$ , where  $f$  is the Darcy's friction factor.

With an electrical network analogy in mind, we introduce a frictional resistance as:

$$\dot{m} = \frac{\Delta P}{R_{f,0}} \quad (2)$$

where  $R_{f,0}$  is the frictional resistance of a smooth microtube of radius  $a$  and length  $L$ :

$$R_{f,0} = \frac{8 \mu L}{\pi \rho a^4} \quad (3)$$

Note that the frictional resistance is not linearly proportional to the radius. The relationship between the frictional resistance, defined in this study, and Darcy's friction factor  $f$  is

$$f = \frac{4 \pi a^3}{\bar{u} L} R_{f,0} \quad (4)$$

The concept of frictional resistance, introduced in Eq. (2), can also be used to construct frictional resistance networks to analyze more complex systems.

## 3 Wall Roughness

Roughness or surface texture can be thought of as the surface deviation from the nominal topography. The term *Gaussian* is

<sup>1</sup>Associate Professor, Director, Microelectronics Heat Transfer Laboratory.

Contributed by the Fluids Engineering Division of ASME for publication in the JOURNAL OF FLUIDS ENGINEERING. Manuscript received March 11, 2005; final manuscript received October 7, 2005. Assoc. Editor: Kenneth Breuer. Paper presented at the 3rd International Conference on Microchannels and Minichannels (ICMM2005), June 13–15, 2005, Toronto, Ontario, Canada.

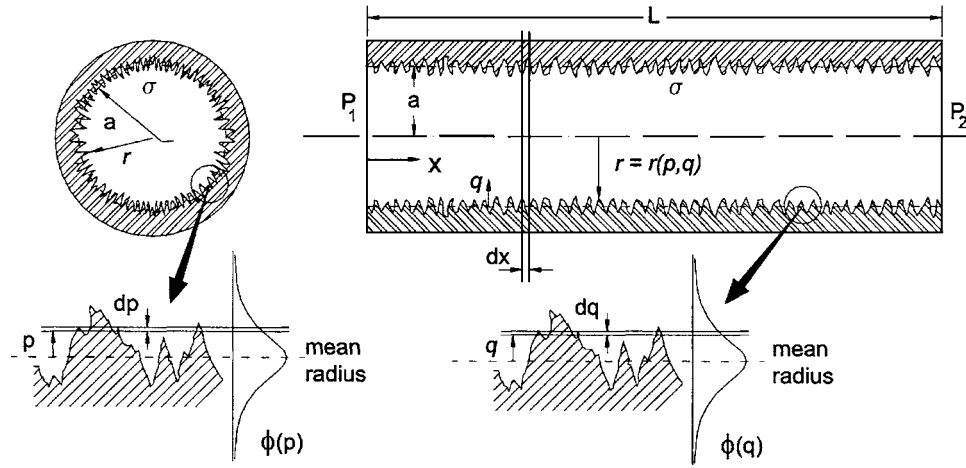


Fig. 1 Random rough microtube: wall roughness and Gaussian distribution

used to describe a surface in which its asperities are isotropic and randomly distributed over the surface. It is not easy to produce a wholly isotropic roughness.

According to Liu et al. [9], five types of instruments are currently available for measuring the surface topography: (i) stylus-type surface profilometer, (ii) optical (white-light interference) measurements, (iii) scanning electron microscope, (iv) atomic force microscope, and (v) scanning tunneling microscope. Among these, the first two instruments are usually used for macro-to-macro asperity measurements, whereas the others may be used for micro- or nanometric measurements. Surface texture is most commonly measured by a profilometer, which draws a stylus over a sample length of the surface. A datum or centerline is established by finding the straight line, or circular arc in the case of round components, from which the mean square deviation is a minimum. The arithmetic average of the absolute values of the measured profile height deviations,  $R_a$ , taken within a sampling length from the graphical centerline [10]. The value of  $R_a$  is

$$R_a = \frac{1}{l} \int_0^l |z(x)| dx \quad (5)$$

where  $l$  is the sampling length in the  $x$  direction and  $z$  is the measured value of the surface heights along this length. When the surface is Gaussian, the standard deviation  $\sigma$  is identical to the rms value  $R_q$ :

$$\sigma = R_q = \sqrt{\frac{1}{l} \int_0^l z^2(x) dx} \quad (6)$$

For a Gaussian surface, it can be shown that the average and rms values are related as follows:

$$R_q \approx \sqrt{\frac{\pi}{2}} R_a \approx 1.25 R_a \quad (7)$$

#### 4 Frictional Resistance of Rough Microtubes

The assumptions of the present model can be summarized as:

- The fully-developed laminar flow is modeled. The fluid is forced to move by a pressure gradient applied to the ends of the microtubes; i.e., pressure-driven flow.
- The fluid is Newtonian and the microtube cross section is circular.
- The microtube walls are rough; the roughness is assumed to be Gaussian, i.e., isotropic in all directions. In addition, there are no *macro* deviations or *waviness* inside the microtubes.

- Rarefaction, compressibility, and slip-on-walls effects are negligible.
- Fluid properties are constant.

Some researchers have reported that the transition from laminar to turbulent flow regimes starts at lower Reynolds numbers in microchannels. However, this early transition has not been observed by Judy et al. [11]. In addition, Obot [12] presented a critical review of published data and concluded that there is hardly any evidence to support the occurrence of transition to turbulence in smooth microchannels for  $Re < 1000$ . Therefore, the focus of this study is on the laminar flow regime and the transition will not be discussed.

Consider a long rough microtube with the mean radius of  $a$  and length  $L \gg a$  (Fig. 1). As shown schematically in the figure, the wall roughness of the microtube is assumed to possess a Gaussian distribution in both the angular and longitudinal directions. Owing to the random nature of the wall roughness, an exact value of the local radius  $r$  cannot be used for rough microtubes. Instead, probabilities of occurring different radii should be computed. A random variable  $p$  is used to represent the deviations of the local radius  $r$  in the angular direction. The standard deviation of  $p$  is the wall roughness  $\sigma_\theta$  and has the following Gaussian distribution:

$$\phi(p) = \frac{1}{\sqrt{2\pi}\sigma_\theta} \exp\left(-\frac{p^2}{2\sigma_\theta^2}\right) \quad (8)$$

The local radius can vary over a wide range of values from much larger to much smaller radii than the mean radius  $a$  (valleys and hills in Fig. 1) with the Gaussian probability distribution shown in Eq. (8). The microtube wall also has roughness in the longitudinal direction  $x$  (see Fig. 1). The variations of the local radius of the microtube  $r$  in the longitudinal direction is shown by another random variable  $q$ , with the same Gaussian distribution as in the angular direction;

$$\phi(q) = \frac{1}{\sqrt{2\pi}\sigma_x} \exp\left(-\frac{q^2}{2\sigma_x^2}\right) \quad (9)$$

The local radius of the microtube can be written as

$$r = a + p + q \quad (10)$$

where  $a$  is the mean statistical value of the local radius  $r$  over the cross sections over the entire length  $L$  of the microtube.

To better understand Eq. (10), consider cross sections of a rough microtube at different longitudinal locations. These cross sections have different mean radii where the probability of these radii occurring can be determined from Eq. (9):  $a+q$ . Meanwhile, the actual radius at each cross section varies around the mean

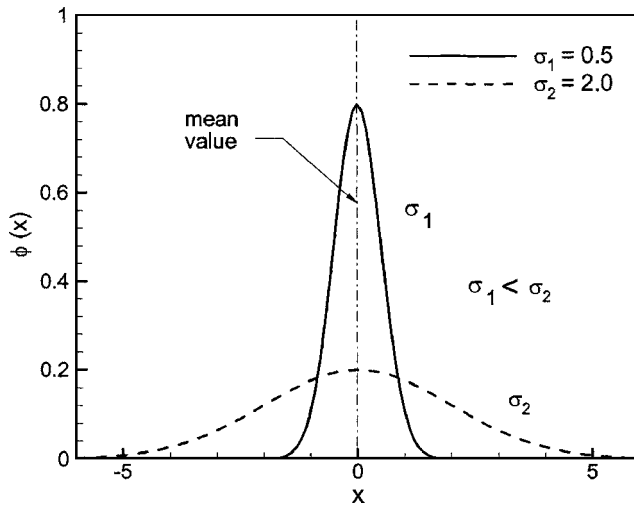


Fig. 2 Gaussian distribution

radius,  $a+q$ , in the angular direction (variations of  $p$ ) with the probability distribution expressed in Eq. (8). Therefore, the local radius  $r$  of a microtube is a function of both random variables  $p$  and  $q$ ; i.e.,  $r=r(p,q)$ . We assume that the local radius is the *superposition* of the two random variables, as shown in Eq. (10). Note that the variables  $p$  and  $q$  are independent. For argument's sake, consider an imaginary case in which a microtube has roughness only in the angular direction; thus, one can write  $r=r(p)$ . As a result, an average of these variables ( $r=a+(p+q)/2$ ) is not correct.

In the general case, the standard deviations  $\sigma_\theta$  and  $\sigma_x$  might be different. However in this study, we assume  $\sigma_\theta=\sigma_x=\sigma$ . This assumption is based on the premise that the texture of microtubes (surface properties) is isotropic which is the case in most MEMS fabrication techniques.

The frictional resistance  $dR_f$  for an infinitesimal element  $dx$  can be written using Eq. (3) as:

$$dR_f = \frac{8\mu dx}{\pi\rho} \int_{-\infty}^{+\infty} \int_{-\infty}^{+\infty} \frac{\phi(p)\phi(q)}{r^4} dp dq \quad (11)$$

Equation (11) considers the probabilities of all values of radius  $r$  occurring according to the Gaussian distribution. It should be noted that it is mathematically possible for the variables  $p$  and  $q$  to

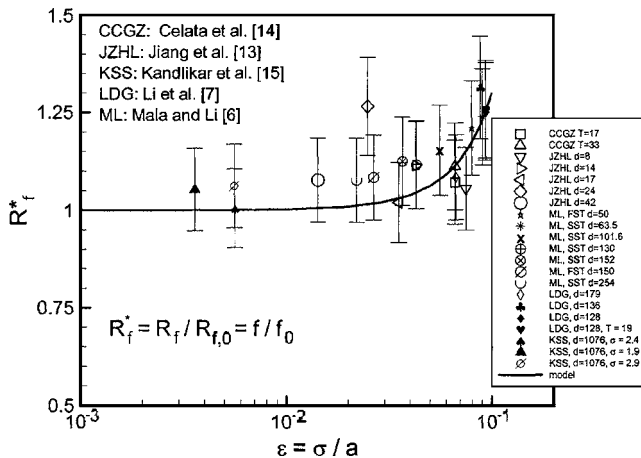


Fig. 3 Effect of relative roughness on pressure drop of microtubes: comparison of present model with all data

have values ranging from  $-\infty$  to  $+\infty$  (see Eqs. (8) and (9)). However, the probability of occurrence of much larger/smaller radii than the mean radius  $a$ , are quite small (see Fig. 2).

The total frictional resistance over the length  $L$  is

$$R_f = \frac{4\mu}{\pi^2 \rho \sigma^2} \int_0^L \int_{-\infty}^{+\infty} \int_{-\infty}^{+\infty} \frac{\phi(p)\phi(q)}{(a+p+q)^4} dp dq dx \quad (12)$$

Equation (12) is used to calculate an *effective* frictional resistance for rough microtubes. Integrating over the length  $L$ , one finds

$$R_f = \underbrace{\frac{8\mu L}{\pi\rho a^4}}_{R_{f,0}} \underbrace{\left\{ \frac{1}{2\pi\sigma^2} \int_{-\infty}^{+\infty} \int_{-\infty}^{+\infty} \frac{\phi(p)\phi(q)}{(1+p/a+q/a)^4} dp dq \right\}}_{\text{effect of wall roughness on frictional resistance}} \quad (13)$$

where  $R_{f,0}$  is the frictional resistance of the smooth microtube, where no roughness exists (see Eq. (3)). Thus, the effect of wall roughness on the frictional resistance can be presented as a normalized frictional resistance or a correction factor, i.e.,  $R_f^* = R_f/R_{f,0}$ . After changing variables and simplifying, one finds

$$R_f^* = \frac{1}{2\pi} \int_{-\infty}^{+\infty} \int_{-\infty}^{+\infty} \frac{\exp(-u^2/2)\exp(-v^2/2)}{[1+\epsilon(u+v)]^4} du dv \quad (14)$$

where  $\epsilon$  is the relative wall roughness

$$\epsilon = \frac{\sigma}{a} \quad (15)$$

Note that in this study, the relative roughness  $\epsilon$ , is defined as the rms wall roughness over the *radius* of the microtube.

The integral in Eq. (14) cannot be solved analytically; thus, it is solved numerically over a range of relative roughness. It can be shown that  $[1+\epsilon(u+v)]^4 \cong (1+\epsilon u)^4(1+\epsilon v)^4$ , where  $\epsilon \ll 1$ ; thus, Eq. (14) can be simplified to

$$R_f^* = \frac{1}{2\pi} \left\{ \int_{-\infty}^{+\infty} \frac{\exp(-u^2/2)}{[1+\epsilon u]^4} du \right\}^2, \quad \epsilon \ll 1 \quad (16)$$

The numerical solution to Eq. (14) is curve fitted and the following correlations can be used to calculate  $R_f^*$ :

$$R_f^* = \begin{cases} \frac{1}{1-23\epsilon^2}, & \epsilon \leq 0.1 \\ \frac{1}{1-50\epsilon^{2.4}}, & 0.1 < \epsilon < 0.15 \end{cases} \quad (17)$$

The maximum relative difference between the numerical values and the above correlation is less than 3%. Note that in the limit where roughness goes to zero, the effective frictional resistance predicted by the present model approaches the Hagen-Poiseuille theory.

Figure 3 illustrates the trend of the normalized frictional resistance  $R_f^*$  as relative roughness  $\epsilon$  is varied. From Eq. (4), it can be seen that the effect of wall roughness on the friction factor  $f$  is the same as the frictional resistance, i.e.,

$$f^* = \frac{f}{f_0} = R_f^* \quad (18)$$

Equations (17) and (18) can be employed to calculate Darcy's friction factor for rough microtubes.

Based on Eq. (17), the effect of roughness is negligible for relative roughness values  $\epsilon < 0.03$ . However, as relative roughness increases the correction factor  $R_f^*$  increases rapidly, e.g., for a microtube with a relative roughness of 0.08, an increase of  $\approx 17\%$  in frictional resistance is predicted by the present model. As  $\epsilon$  increases to approximately 0.2, the normalized frictional resistance approaches infinity.

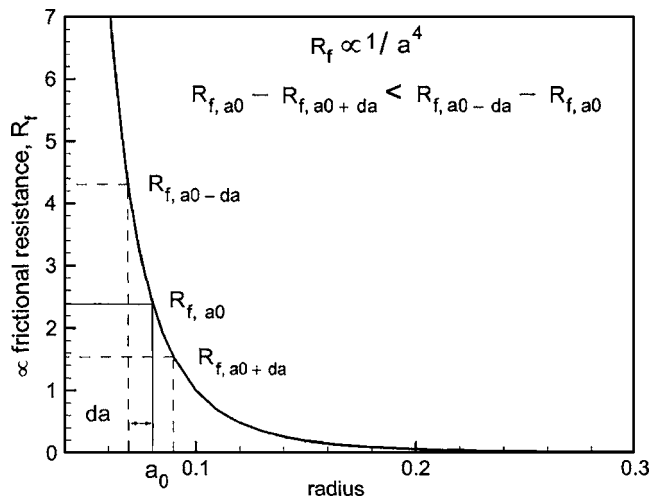


Fig. 4 Relationship between frictional resistance and radius of rough microtubes

It should be noted that the relative roughness of 0.2 is extremely high—imagine a microtube where the standard deviation of its wall roughness is 1/5 of its radius. It is also worth noting that in the Gaussian distribution as the standard deviation increases, the probability of occurring radii with larger deviations from the mean radius becomes higher (see Fig. 2). In other words, in rougher microtubes (higher values of  $\sigma$ ) the probability of occurring smaller radii is higher, which leads to higher pressure drops.

Increasing roughness, while all other parameters are kept constant, results in an increase in the frictional resistance or equivalently the pressure drop (see Eq. (17)). We know that by assuming the Gaussian distribution, the probabilities of having smaller and/or larger radii microtubes (than the mean radius  $a$ ) are identical; the mean statistical radius of the microtube also remains unchanged as the roughness is increased. The question may then arise as to why the frictional resistance increases as roughness increases. The answer to this question lies in the relationship between the frictional resistance and the radius of microtube (Eq. (3)). The frictional resistance is inversely proportional to the radius to the fourth power:  $R_f \propto 1/a^4$ . Figure 4 illustrates the frictional resistance as a function of the radius. The frictional resistance of a slightly smaller radius ( $a_0 - da$ ) is much larger than the resistance of a slightly larger radius ( $a_0 + da$ ) (see Fig. 4). Therefore, the resistance of smaller radii microtubes controls the effective frictional resistance and the effective frictional resistance increases as a microtube becomes rougher.

## 5 Comparison with Data

The present model is compared against experimental data conducted by several researchers. A constant roughness value is used for the same microtube material for all radii reported in each reference. In other words, the roughness is assumed *not* to be a function of the microtube radius. This assumption may not be strictly correct, unfortunately, none of the available experimental studies reported the wall roughness for different radii of microtubes. Different values for the uncertainty of the experimental data were reported by different researchers, in the vicinity of 10%; thus, a constant error bound of 10% is considered for all data.

Li et al. [7] tested glass, silicon, and stainless steel microtubes with diameters ranging from 79.9 to 166.3  $\mu\text{m}$ , from 100.25 to 205.3  $\mu\text{m}$ , and from 128.76 to 179.8  $\mu\text{m}$ , respectively. The Reynolds number was varied over  $500 < Re < 2500$ . To determine the wall conditions, the three types of microtubes were milled open along the axial direction. The wall roughness was measured using

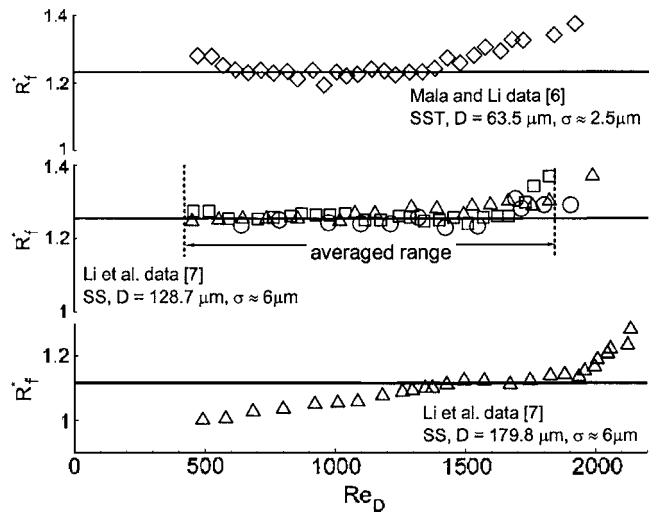


Fig. 5 Comparison of present model to Li et al. [7] and Mala and Li [6] data

a Talysurf-120 profilometer. The wall roughness of glass and silicon microtubes were reported in order of 0.05  $\mu\text{m}$ ; thus the glass and the silicon microtubes can be considered as smooth microtubes. However, the stainless steel microtubes exhibited a relatively large wall roughness. They [7] did not report the exact value of  $R_q$  or  $R_a$  for wall roughness; only a “peak-valley roughness” in the order of  $\approx 5.5 \mu\text{m}$  was reported for stainless steel microtubes. Through experiments, Li et al. [7] showed that for glass and silicon microtubes the conventional theory in the laminar regime holds. For stainless steel microtubes the friction factors were higher than the prediction of the classical theory.

Mala and Li [6] studied experimentally the flow of deionized water through circular microtubes of fused silica and stainless steel with Reynolds numbers in the range  $100 < Re < 2500$  and with diameters ranging between 50 to 254  $\mu\text{m}$ . They reported a strange nonlinear trend between pressure drop and flow rate for low Reynolds numbers, and that the friction factors were consistently higher than the conventional values.

Figure 5 shows the comparison between the present model, Eq. (17), and two sets of data from Li et al. [7] and one set of data from Mala and Li [6]. As can be seen, the model agrees well with these data.

Jiang et al. [13] studied the trend of water flow through glass microtubes. Their circular microtubes were fabricated by the glass drawn process, with wall roughness in the order of 0.3  $\mu\text{m}$ . The microtubes diameters ranged from 8 to 42  $\mu\text{m}$  with Reynolds numbers in the range  $0.12 < Re < 3$ . The range of the Reynolds number, in which their experiments were conducted, was very low. However, they did not report any trends similar to those of Mala and Li [6]. Figure 6 shows the comparison between the present model and a set of the [13] data.

Celata et al. [14] performed an experimental analysis of the friction factor in stainless steel capillary tubes with a diameter of 130  $\mu\text{m}$  with R114 as the fluid with Reynolds numbers in the range  $100 < Re < 8000$ . Their reported values of  $R_a$  have been converted to  $\sigma = R_q$ , using Eq. (7), to be used in the comparison.

Kandlikar et al. [15] investigated experimentally the role of the wall roughness on the pressure drop in two microtubes with Reynolds numbers in the range  $500 < Re < 2500$  and with different diameters 1067 and 620  $\mu\text{m}$ . The wall roughness of the microtube walls was changed by etching with an acid solution. A micrograph scan of the microtubes was used to measure the average roughness  $R_a$  (see Eq. (5)). Their reported values of  $R_a$  have been converted to  $\sigma = R_q$ , using Eq. (7), to be used in the comparison.

The frictional resistance constant,  $C = f Re_D$ , is not a function of



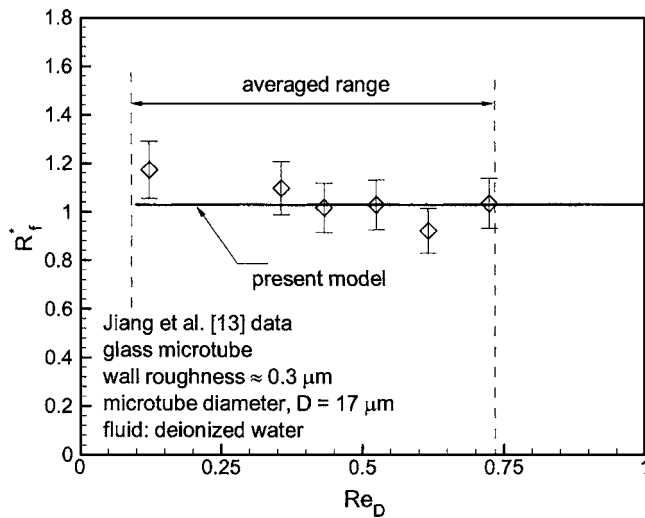


Fig. 6 Comparison of present model to Jiang et al. [13]

Reynolds number and remains unchanged for the laminar regime. Therefore, the experimental data are averaged over the laminar region; the transitional data are *not* included in the comparison. For each data set, the relative roughness is calculated using  $\epsilon = \sigma/a$ . As a result, for each experimental data set, a relative roughness and a normalized frictional resistance can be obtained, dashed lines in Figs. 5 and 6 demarcate the averaged ranges.

Figure 3 shows the comparison between the experimental data (normalized frictional resistance as a function of relative roughness) and the present model (Eq. (17)). As previously mentioned, the nonlinear trend of Mala and Li [6] data (at low Reynolds numbers) has not been observed by any other researchers. Therefore, those data points are not included in the averaged values shown in Fig. 3. The agreement between the model and the data is relatively good; within the 10% for most of data points. More importantly, the present model captures the trends of the data as relative roughness increases.

## 6 Summary and Conclusions

The influence of wall roughness on the laminar, fully developed, incompressible flow in microtubes is studied and a new model is proposed. The concept of frictional resistance is introduced and its relation to the Darcy's friction coefficient is derived.

The present model assumes an isotropic Gaussian distribution for wall roughness. In addition, the rarefaction, compressibility, and slip-on-wall effects are assumed to be negligible. Owing to the random nature of the wall roughness, an exact value of the local radius cannot be used for rough microtubes. Instead, probabilities of different radii occurring should be computed. Two independent random variables are considered to account for the deviations of the local radius in the angular and longitudinal directions. The local radius of a microtube is a function of these two random variables. In the present model, the local radius is assumed to be the superposition of the two random variables. The effect of wall roughness on the frictional resistance is presented as a normalized frictional resistance or a correction factor; the final results are reported in the form of a compact correlation. It is found that the effect of roughness is to increase the pressure drop in microtubes. The effect of roughness can be neglected when relative roughness is less than 3%. It is observed that the constant in the conventional frictional resistance,  $C = f \text{Re}_D$ , is a function of relative roughness, i.e.,  $C = C(\epsilon)$ . The published experimental data, in which the roughness is reported, are collected and compared with the present model. The present model exhibits the influence of roughness and predicts the pressure drop within the uncertainty of data.

There is a need for carefully designed experimentation aimed at more comprehensive wall roughness and pressure drop measurements. For most conventional microtubes, the relative roughness is small, in the order of a few percent. According to the model, the increase in the pressure drop for these microtubes are within the uncertainty of the current experimental arrangements, i.e., 10%. This makes the validation of the present model a difficult task for relatively smooth microtube.

## Acknowledgment

The authors gratefully acknowledge the financial support of the Centre for Microelectronics Assembly and Packaging, CMAP and the Natural Sciences and Engineering Research Council of Canada, NSERC. Our thanks go to Mr. K. Narimani for his helpful comments on Sec. 4.

## Nomenclature

- $a$  = mean radius of rough microtube, m
- $C$  = Darcy's friction coefficient,  $f \text{Re}_D$
- $D$  = microtube inside diameter, m
- $f$  = Darcy's friction factor, (-)
- $f^*$  = normalized friction factor,  $f/f_0$
- $L$  = microtube length, m
- $\dot{m}$  = mass flow rate, kg/s
- $p, q$  = random variables, m
- $R_a$  = arithmetic average wall roughness, m
- $r$  = radius, m
- $\text{Re}_D$  = Reynolds number,  $\rho \bar{u} D / \mu$
- $R_f$  = frictional resistance,  $\text{m}^{-1} \text{s}^{-1}$
- $R_f^*$  = normalized frictional resistance,  $R_f/R_{f,0}$
- $R_q$  = rms wall roughness, m
- $T$  = mean fluid temperature, °C
- $\bar{u}$  = mean fluid velocity, m/s
- $z$  = measured values of surface heights, m

## Greek

- $\epsilon$  = relative roughness,  $\equiv \sigma/a$
- $\rho$  = fluid density,  $\text{kg}/\text{m}^3$
- $\mu$  = fluid viscosity,  $\text{kg}/\text{m s}$
- $\sigma$  = roughness standard deviation, m
- $\Delta P$  = pressure gradient, Pa

## Subscripts

- 0 = reference value, smooth microtube
- $\theta$  = in angular direction
- $x$  = in longitudinal direction

## References

- [1] Sobhan, C. B., and Garimella, S. V., 2001, "A Comparative Analysis of Studies on Heat Transfer and Fluid Flow in Microchannels," *Microscale Thermophys. Eng.*, **5**(4), pp. 293–311.
- [2] Morini, G. L., 2004, "Single-Phase Convective Heat Transfer in Microchannels: A Review of Experimental Results," *Int. J. Therm. Sci.*, **43**, pp. 631–651.
- [3] Tuckerman, D. B., 1984, *Heat Transfer Microstructures for Integrated Circuits*, Ph.D. thesis, Stanford University, Dept. of Electrical Eng., California.
- [4] Pfahler, J., Harley, J., Bau, H. H., and Zemel, J., 1990, "Liquid and Gas Transport in Small Channels," *ASME Dynamic Systems and Control Division—DSC, Microstructures, Sensors, and Actuators*, Vol. **19**, pp. 149–157.
- [5] Pfahler, J., Harley, J., and Zemel, H. H., 1991, "Gas and Liquid Flow in Small Channels," *ASME Dynamic Systems and Control Division—DSC, Microstructures, Sensors, and Actuators*, Vol. **32**, pp. 49–60.
- [6] Mala, G. M., and Li, D. Q., 1999, "Flow Characteristics of Water in Microtubes," *Int. J. Heat Fluid Flow*, **20**(2), pp. 142–148.
- [7] Li, Z., Du, D., and Guo, Z., 2003, "Experimental Study on Flow Characteristics of Liquid in Circular Microtubes," *Microscale Thermophys. Eng.*, **7**(3), pp. 253–265.

- [8] Kleinstreuer, C., and Koo, J., 2004, "Computational Analysis of Wall Roughness Effects for Liquid Flow in Micro-conduits," *ASME J. Fluids Eng.*, **126**, pp. 1–9.
- [9] Liu, G., Wang, Q., and Ling, C., 1999, "A Survey of Current Models for Simulating Contact Between Rough Surfaces," *Tribol. Trans.*, **42**(3), pp. 581–591.
- [10] ANSI b46.1, 1985, "Surface texture: Surface Roughness, Waviness and Lay."
- [11] Judy, J., Maynes, D., and Webb, B. W., 2002, "Characterization of Frictional Pressure Drop for Liquid Flows Through Microchannels," *Int. J. Heat Mass Transfer*, **45**, pp. 3477–3489.
- [12] Obot, N. T., 2002, "Toward a Better Understanding of Friction and Heat/Mass Transfer in Microchannels—A Literature Review," *Microscale Thermophys. Eng.*, **6**, pp. 155–173.
- [13] Jiang, X. N., Huang, X. Y., and Liu, C. Y., 1997, "Laminar Flow Through Microchannels Used for Microscale Cooling Systems," *IEEE CPMT Electronic Packaging Technology Conference*, pp. 119–122.
- [14] Celata, G., Cumo, M., Guglielmi, M., and Zummo, G., 2002, "Experimental Investigation of Hydraulic and Single Phase Heat Transfer in 0.130 mm Capillary Tube," *Microscale Thermophys. Eng.*, **6**, pp. 85–97.
- [15] Kandlikar, S. G., Joshi, S., and Tian, S., 2001, "Effect of Channel Roughness on Heat transfer and Fluid Flow Characteristics at Low Reynolds Numbers in Small Diameter Tubes," *Proceedings of the National Heat Transfer Conference, ASME*, Vol. **2**, pp. 1609–1618.